Phosphoglycerate kinase acts as a futile cycle at high temperature

Kouril, Theresa; Eicher, Johann J; Siebers, Bettina; Snoep, J.L.

published in
Microbiology
2017

DOI (link to publisher)
10.1099/mic.0.000542

MICROBIOLOGY

RESEARCH ARTICLE

Kouril *et al.*, *Microbiology* 2017;163:1604–1612
DOI 10.1099/mic.0.000542

MICROBIOLOGY SOCIETY

Phosphoglycerate kinase acts as a futile cycle at high temperature

Theresa Kouril,[1,2] Johann J. Eicher,[2] Bettina Siebers[1] and Jacky L. Snoep[2,3,4,*]

Abstract

In (hyper)thermophilic organisms metabolic processes have to be adapted to function optimally at high temperature. We compared the gluconeogenic conversion of 3-phosphoglycerate via 1,3-bisphosphoglycerate to glyceraldehyde-3-phosphate at 30 °C and at 70 °C. At 30 °C it was possible to produce 1,3-bisphosphoglycerate from 3-phosphoglycerate with phosphoglycerate kinase, but at 70 °C, 1,3-bisphosphoglycerate was dephosphorylated rapidly to 3-phosphoglycerate, effectively turning the phosphoglycerate kinase into a futile cycle. When phosphoglycerate kinase was incubated together with glyceraldehyde 3-phosphate dehydrogenase it was possible to convert 3-phosphoglycerate to glyceraldehyde 3-phosphate, both at 30 °C and at 70 °C, however, at 70 °C only low concentrations of product were observed due to thermal instability of glyceraldehyde 3-phosphate. Thus, thermolabile intermediates challenge central metabolic reactions and require special adaptation strategies for life at high temperature.

INTRODUCTION

Highly conserved core reaction networks exist through organisms of all domains of life, even though these organisms may inhabit and have adapted to sometimes very different environmental conditions. For instance, when we look at the metabolism of (hyper)thermophiles, we see that the catalysts have adapted (to improve stability at high temperatures), but the reaction steps and intermediates in pathways are largely conserved [1, 2].

Glycolysis is one of those highly conserved pathways and plays an important role in providing cells with the necessary building blocks and adenosine triphosphate (ATP) for biosynthesis. In the absence of glucose, the pathway operates in the reverse direction to maintain the availability of building blocks such as glucose 6-phosphate, and to ensure the reversibility of thermodynamically unfavourable reactions, alternative enzymes are expressed under gluconeogenic conditions for three (phosphofructokinase, pyruvate kinase, glucokinase) of the four kinases, but not for the phosphoglycerate kinase (PGK) in the classic Embden–Meyerhof–Parnas pathway. Such antagonistic enzymes, acting as kinase/phosphatase or kinase/synthetase couples, could potentially lead to futile cycles in the pathway if they are active simultaneously. To prevent this, the antagonistic enzyme-reaction couples are often highly regulated and conditionally expressed (e.g. [3]).

Ultimately the Gibbs free energy needed for ATP synthesis in glycolysis is derived from chemical conversions leading to intermediates with a high chemical potential. The oxidative phosphorylation of glyceraldehyde 3-phosphate (GAP) to 1,3-bisphosphoglycerate (BPG) combined with the PGK are particularly important, as these reactions are responsible for the net production of ATP in the pathway. The high chemical potential of intermediates can make these compounds unstable, a characteristic well known for BPG. Instability of pathway intermediates with high chemical potential could have serious consequences for substrate level phosphorylation.

The high chemical potential of BPG and the resulting high Keq of PGK, led us to study the PGK-GAPDH reaction steps of gluconeogenesis paying specific attention to the thermal stability of BPG and the thermodynamics of its formation. We compared GAPDH and PGK kinetics in the gluconeogenic direction for yeast (optimal growth at 25–30 °C, pH 7) and for the thermoacidophilic Archaeon *Sulfolobus solfataricus* (optimal growth temperature of 70–85 °C, pH 3). We show that BPG rapidly dephosphorylates to 3 PG at 70 °C, leading to futile cycling of ATP by PGK, while at

Received 25 May 2017; Accepted 17 September 2017
Author affiliations: [1]Molecular Enzyme Technology and Biochemistry (MEB), BiofilmCentre, Faculty of Chemistry, University of Duisburg-Essen, Duisburg, Germany; [2]Department of Biochemistry, Stellenbosch University, Private Bag X1, Matieland 7602, South Africa; [3]Molecular Cell Physiology, Vrije Universiteit Amsterdam, Amsterdam, The Netherlands; [4]MIB, University of Manchester, Manchester, UK.
***Correspondence:** Jacky L. Snoep, jls@sun.ac.za
Keywords: gluconeogenesis; thermophiles; NMR spectroscopy; kinetic modelling; thermal degradation; archaea.
Abbreviations: 3-PG, 3-phosphoglycerate; BPG, 1,3-bisphosphoglycerate; GAP, glyceraldehyde 3-phosphate; GAPDH, glyceraldehyde 3-phosphate dehydrogenase; GDH, glucose dehydrogenase; PGK, phosphoglycerate kinase; PK, pyruvate kinase; Sso, S. solfataricus; TEP, triethyl phosphate.
Supplementary material is available with the online version of this paper.

moderate temperatures BPG is much more stable, but a strong thermodynamic feedback prevents conversion of 3 PG to BPG (unless strongly 'pushed' by high ATP/ADP ratios). At both temperatures the combined GAPDH-PGK reaction steps can overcome the thermodynamic constraint created by the high chemical potential of BPG.

METHODS

Assays at 70 °C with *S. solfataricus* enzymes

Recombinant *S. solfataricus* PGK (Sso-PGK), GAPDH (Sso-GAPDH), glucose dehydrogenase (Sso-GDH) and pyruvate kinase (Sso-PK) were prepared as reported previously [4]. All assays were performed at 70 °C in 0.1 M Tris/HCl (pH 6.5) containing 20 mM $MgCl_2$. Reactions were initialized by the addition of 3 PG. Samples were withdrawn at regular time points and metabolite concentrations were quantified as described previously [4] or changes in phosphorylated metabolite concentrations were followed online using ^{31}P-NMR (section 'NMR analyses').

For the PGK incubation with offline enzymatic quantification of intermediates, 3.4 μg ml^{-1} Sso-PGK was incubated with 4 mM 3 PG, 10 mM ATP, 2 mM PEP and 40 μg ml^{-1} Sso-PK. The PGK NMR analysis was performed in a total volume of 1 ml in the presence of 10 mM ATP, 5 mM PEP 10 % D_2O 14 μg ml^{-1} Sso-PGK, and 80 μg ml^{-1} Sso-PK or 28 μg ml^{-1} Sso-PGK, and 160 μg ml^{-1} Sso-PK, respectively. Assays were performed in the absence and presence of the ATP recycling system (i.e. PEP and PK).

For the PGK-GAPDH incubations at 70 °C, 42.1 μg ml^{-1} Sso-GAPDH was incubated together with 3.4 μg ml^{-1} Sso-PGK in an assay mixture containing 3 mM 3 PG, 10 mM ATP, 5 mM PEP, 40 μg ml^{-1} Sso-PK, 0.2 mM NADPH, 10 mM glucose and 3 μg ml^{-1} Sso-GDH. Samples were withdrawn after 0, 20, 40, 60, 80, 100 and 120 min and metabolite concentrations were quantified by enzymatic methods [4].

Assays at 30 °C with *Saccharomyces cerevisiae* enzymes

Assays were performed at 30 °C, using enzymes purchased from Sigma-Aldrich (Taufkirchen, Germany). The assay mixtures were pre-incubated for 3 min to reach 30 °C in 0.1 M Tris/HCl (pH 7) and started by the addition of 3 PG.

For the PGK incubation, 3.9 μg ml^{-1} PGK (yeast) was incubated in the presence of 10 mM ATP, 20 mM $MgCl_2$, 32 U ml^{-1} pyruvate kinase (rabbit muscle) and 5 mM PEP. The reaction was started by the addition of 4 mM 3 PG and aliquots (5 μl) were withdrawn at 0, 5, 10, 20, 30 min and metabolite concentrations were determined.

For the PGK-GAPDH incubation, 0.0324 μg ml^{-1} PGK (yeast) was incubated with 0.052 mg ml^{-1} GAPDH (yeast) in an assay mixture containing 0.1 M Tris/HCl (pH 7), 3 mM 3 PG, 10 mM ATP, 20 mM $MgCl_2$, 5 mM PEP, 32 U ml^{-1} pyruvate kinase (rabbit muscle), 0.2 mM NADPH, 10 mM glucose and 30 U ml^{-1} glucose dehydrogenase (Pseudomonas). Samples of 5 μl were withdrawn after 0, 20, 40, 60, 80, 100, 120 and 150 min.

The intermediate concentrations for the yeast incubations were determined at 70 °C, using thermophilic enzymes that were enriched from recombinant extract by heat precipitation: (a) BPG concentration was determined by adding the 5 μl sample to a pre-heated solution at 70 °C (500 μl total volume), which contains 0.1 mM NADPH, 0.1 M Tris/HCl (pH 6.5, 70 °C), 10 mM $MgCl_2$, 5 mM ATP and 50 μg Sso-GAPDH. (b) After completion of the GAPDH reaction 25 μg *Thermoproteus tenax* PGK was added to determine the 3 PG concentration. (c) GAP was quantified at 70 °C by adding the 5 μl sample to 0.1 M Tris/HCl (pH 6.5, 70 °C), 2 mM $NADP^+$, 0.1 mM glucose 1-phosphate in the presence of 20 μg Sso-GAPN (non-phosphorylating glyceraldehyde 3-phosphate dehydrogenase). (d) The PK-dependent formation of pyruvate was assayed by addition of 5 μl aliquots to 0.1 mM NADH in 0.1 M Tris/HCl (pH 7, room temperature) in the presence of lactate dehydrogenase. For ^{31}P NMR analyses 38 μg ml^{-1} PGK (yeast) was incubated at 30 °C in 0.1 M Tris/HCl (total volume of 1 ml) in the presence of 20 m $MgCl_2$, 10 mM ATP, 5 mM PEP 10 % D_2O, 100 μg ml^{-1} PK (rabbit muscle) and the reaction was initiated by adding 5 mM 3 PG.

NMR analyses

Two forms of acquisition were employed for monitoring reactions with NMR: a rapid acquisition for high-resolution spectra, and a slow acquisition for quantitative results, allowing all nuclei to fully relax. All reactions were monitored using ^{31}P NMR at 30 °C on a 400 MHz spectrometer (Varian/Agilent), with inverse-gated proton-decoupling.

During the rapid high-resolution experiments, 48 transients were collected per free induction decay (FID), with a repetition time of 2 s (1 s acquisition; 1 s relaxation). During the slow quantitative experiments, two transients were collected per FID, with a repetition time of 41.6 s (1.6 s acquisition; 40 s relaxation).

5 mM triethyl phosphate (TEP) was included in all incubations as a metabolically inert internal standard. Locking and shimming were first performed on a reaction vial lacking enzymes, after which these were included, and the reaction progress monitored.

Specific activities of *Saccharomyces cerevisiae* enzymes

Specific activities of the yeast PGK and GAPDH in the gluconeogenic direction were determined under the same conditions as the incubations' assays, except that no NADH recycling enzyme was added, and 10 mM 3 PG was used. For the PGK assay 0.2 μg ml^{-1} PGK (yeast) and 0.48 mg ml^{-1} GAPDH (yeast) was used and a specific activity of 1095 U mg^{-1} PGK was measured. For the GAPDH assay 39 μg ml^{-1} PGK (yeast) and 6 μg ml^{-1} GAPDH (yeast) was used and a specific activity of 15.4 U mg^{-1} GAPDH was measured. These activities were converted to Vmax values

of 1182.6 U mg^{-1} for PGK and 20.02 U mg^{-1} for GAPDH using the rate equations given in [5].

Determination of the half-life time of BPG

BPG was synthesized with yeast PGK using the assay as described above (section 'Assays at 30 °C with *Saccharomyces cerevisiae* enzymes'). The synthesis reaction was stopped by the addition of acetone (1 : 1) and subsequent incubation at −80 °C for 20 min. After centrifugation (12 000 ***g***, 20 min, 4 °C) the supernatant was transferred in a fresh tube and the acetone was removed using speed vac centrifugation at room temperature. In total, 100 µl of the sample was added to a pre-incubated (3 min, 70 °C) mixture of 900 µl 0.1 M Tris/HCl (pH 6.5 at 70 °C) containing 20 mM $MgCl_2$. Samples (150 µl) were withdrawn and stored on ice after various incubation times (0, 30, 60, 90, 120, 150 s). BPG and 3 PG concentrations were determined enzymatically at 25 °C. Overall, 25 µl of the reaction mixture was transferred to 0.1 M Tris/HCl (pH 7, room temperature) containing 2 mM ATP, 10 mM $MgCl_2$, 0.1 mM NADH and 10 U GAPDH (rabbit muscle) in 500 µl total volume. After completion of the GAPDH reaction, 6 U PGK (yeast) was added to determine 3 PG concentrations.

Computational methods

For simulation of the *S. solfataricus* GAPDH activity, we adapted the original rate equation and parameter values [4]. The enzyme was now characterized in the Tris/HCl incubation buffer, which resulted in significantly different kinetics (see Fig. S1, available in the online Supplementary Material). For the PGK we used the original equation, but refitted the kinetic parameters for BPG (and ADP). For a full description of the adaptations made to the enzyme kinetics, and fitting and validation results see Fig. S2, here we only give the rate equations and parameter values that were used.

For the Sso-GAPDH (equation 1):

$$\nu\mathrm{GAPDH} = \frac{\frac{V_{\mathrm{Mf}}\,(\mathrm{BPG\ NADPH})}{K_{\mathrm{M,BPG}}\,K_{\mathrm{M,NADPH}}} - \frac{V_{\mathrm{Mr}}\,(\mathrm{Pi\ GAP\ NADP})}{K_{\mathrm{M,Pi}}\,K_{\mathrm{M,GAP}}\,K_{\mathrm{M,NADP}}}}{\left(1+\frac{\mathrm{NADP}}{K_{\mathrm{M,NADP}}}+\frac{\mathrm{NADPH}}{K_{\mathrm{M,NADPH}}}\right)\left(\frac{\mathrm{BPG}}{K_{\mathrm{M,BPG}}}+\left(1+\frac{\mathrm{GAP}}{K_{\mathrm{M,GAP}}}\right)\left(1+\frac{\mathrm{Pi}}{K_{\mathrm{M,Pi}}}\right)\right)}$$

With the kinetic parameters as listed in Table 1.

For the Sso-PGK (equation 2):

$$\nu\mathrm{PGK} = \frac{\frac{V_{\mathrm{Mf}}\,(\mathrm{ATP\ 3PG})}{K_{\mathrm{M,ATP}}\,K_{\mathrm{M,3PG}}} - \frac{V_{\mathrm{Mr}}\,(\mathrm{ADP\ BPG})}{K_{\mathrm{M,ADP}}\,K_{\mathrm{M,BPG}}}}{\left(1+\frac{\mathrm{ADP}}{K_{\mathrm{i,ADP}}}\right)\left\{1+\frac{\mathrm{3PG}}{K_{\mathrm{M,3PG}}}\left(1+\frac{\mathrm{ATP}}{K_{\mathrm{M,ATP}}}\right)+\frac{\mathrm{BPG}}{K_{\mathrm{M,BPG}}}\left(1+\frac{\mathrm{ADP}}{K_{\mathrm{M,ADP}}}\right)\right\}}$$

With the kinetic parameters as listed in Table 2.

For yeast GAPDH and PGK we used the rate equations and parameter values as described in [5], with the Vm values as reported above (section 'Specific activities of *Saccharomyces cerevisiae* enzymes').

All numerical analyses were performed in Mathematica [6]. The full model description and detail on the numerical procedures is available in the online Supplementary Material. The models are available on JWS Online as kouril4, kouril5, kouril6, kouril7, kouril8, and kouril9, (via https://jjj.bio.vu.nl/models/?id=kouril) and all data files are available on the FAIRDOMHub (https://fairdomhub.org/investigations/156).

Table 1. Kinetic parameters of the glyceraldehyde 3-phosphate dehydrogenase of *S. solfataricus*, as indicated in equation 1

	Value	Units
V_{Mf}	23.40	U mg^{-1}
V_{Mr}	35.87	U mg^{-1}
$K_{\mathrm{M,GAP}}$	3.09	mM
$K_{\mathrm{M,NADP}}$	0.20	mM
$K_{\mathrm{M,Pi}}$	112.4	mM
$K_{\mathrm{M,BPG}}$	0.09	mM
$K_{\mathrm{M,NADPH}}$	0.09	mM

RESULTS AND DISCUSSION

PGK catalyses the reversible reaction: 3-PG+ATP⟷BPG +ADP (Fig. 1a). The chemical equilibrium of the reaction lies strongly towards 3 PG (Keq=1/3200, $\Delta G^0$18.8 kJ mol^{-1} (values taken from [5]). By incubating yeast PGK in the presence of ATP, 3 PG and $MgCl_2$ at 30 °C, hardly any 3 PG was converted to BPG (Fig. 1a, open symbols). However, in the presence of an effective ATP recycling system (keeping ADP levels negligibly low) yeast PGK readily phosphorylated 3 PG to BPG at 30 °C (Fig. 1a, closed symbols), showing that PGK was strongly limited in its conversion of 3 PG to BPG due to thermodynamic constraints. Even in the presence of the ATP recycling mechanism the reaction did not run to completion (Fig. 1a). During 3 PG conversion, BPG and ADP were produced at equal rates (the latter was monitored via pyruvate production in the recycling system).

In addition to enzymatic analyses, we applied ^{31}P-NMR spectroscopy to confirm BPG formation, and to unravel its spectra. The NMR spectra showed the formation of three peaks, two of which were assigned to BPG1 and BPG3, and a third peak corresponded with phosphate (Fig. 1b–d). It has been reported previously that BPG decays at 60 °C with a half-life of 1.6 min [7], however, no studies of the decay products are available. The formation of phosphate strongly suggests that BPG dephosphorylates to 3 PG (which is stable at high temperature, i.e. half-life of 18 h at 88 °C [8]). This

Table 2. Kinetic parameters of the phosphoglycerate kinase of *S. solfataricus*, as indicated in equation 2

	Value	Units
V_{Mf}	17.21	U mg^{-1}
V_{Mr}	37.96	U mg^{-1}
$K_{\mathrm{M,ADP}}$	0.37	mM
$K_{\mathrm{M,BPG}}$	0.008	mM
$K_{\mathrm{i,ADP}}$	1.02	mM
$K_{\mathrm{M,ATP}}$	9.31	mM
$K_{\mathrm{M,3PG}}$	0.57	mM

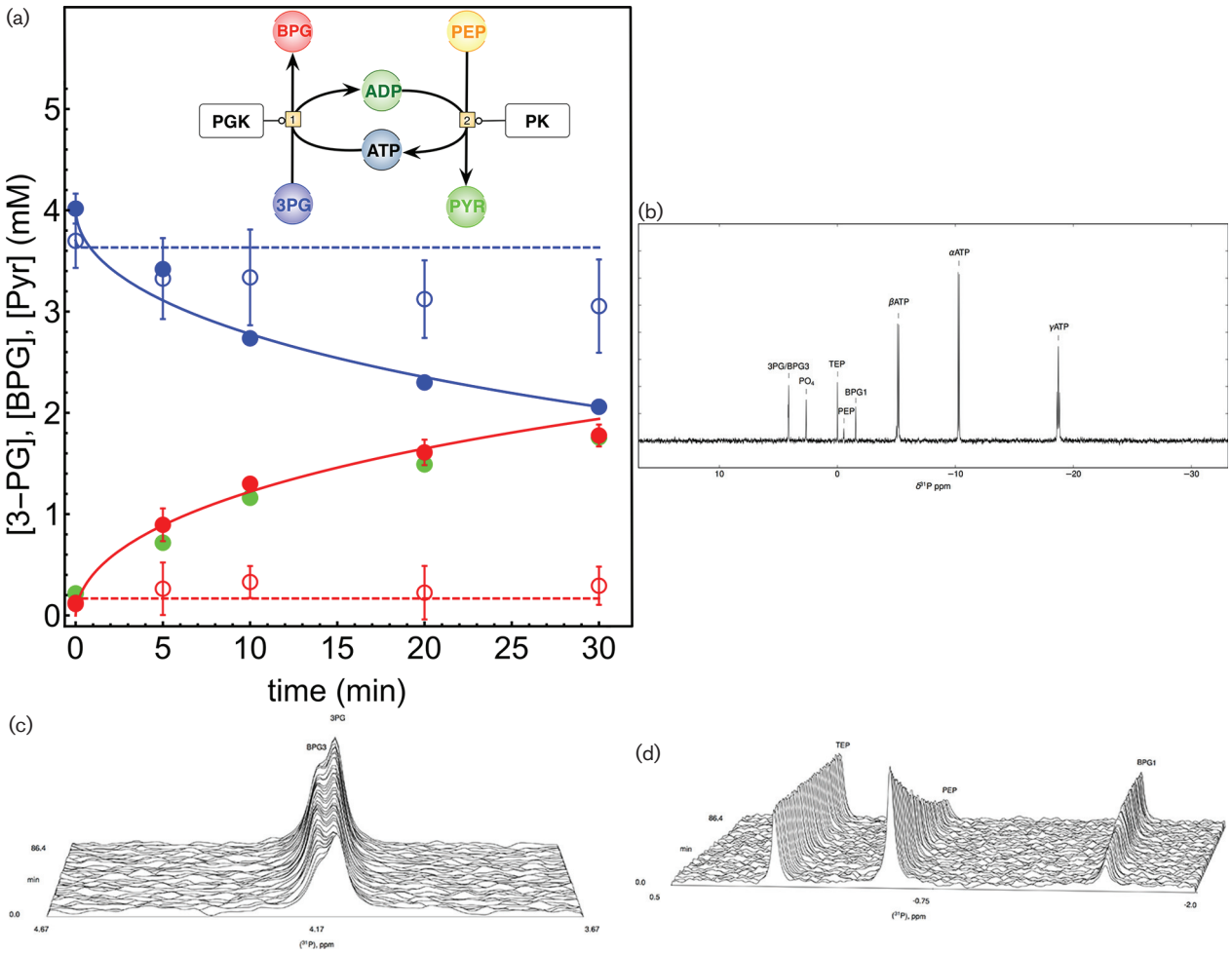

Fig. 1. PGK reaction at 30 °C. Yeast PGK (3.9 µg ml^{-1}) was incubated at 30 °C, (Fig. 1a) in the presence (closed symbols, full lines) or absence (open symbols, dashed lines) of the ATP recycling system (reaction 2 in insert), and the conversion of 3 PG (blue symbols) to BPG (red symbols) was followed. Lines (coloured correspondingly to the symbols) in the figures are model predictions for the respective systems (see Methods and the online Supplementary Material for details). Pyruvate production (green symbols) via the ATP recycling system reflects ADP production. Model simulations in Fig. 1(a) were made with the model kouril4.xml and can be reproduced with the following link: https://jjj.bio.vu.nl/models/experiments/kouril2017_fig1a/simulate. Fig. 1(b–d) ^{31}P NMR spectra (see Methods for details) in the presence of 38 µg ml^{-1} yeast PGK.

was tested by heating-up the BPG (synthesized with yeast PGK at 30 °C) and following the reduction in BPG and increase in 3 PG concentrations over time. We confirmed that BPG dephosphorylates quickly and solely to 3 PG with a half-life time of 56.5 s at 70 °C (Fig. 2).

This poses an interesting challenge for the PGK-catalysed conversion of 3 PG to BPG at high temperature; PGK activity combined with BPG degradation creates a 'one enzyme' futile cycle that effectively hydrolyses ATP. Exactly this behaviour was observed when incubating the *S. solfataricus* PGK at 70 °C (see Fig. 3a). Any 3 PG conversion to BPG was negated by BPG degradation, keeping the 3 PG and BPG concentrations constant, with a net hydrolysis of ATP, which was monitored by pyruvate production via the ATP recycling mechanism (see Fig. 3a, c, d). In the absence of the ATP recycling reaction, a low ATP hydrolysis activity was observed (see Fig. 3b), which increased strongly when ATP was recycled (see Fig. 3d). The net rate of ATP hydrolysis was not proportional to the PGK concentration, i.e. when halving the PGK concentration from 28 µg ml^{-1} to 14 µg ml^{-1}, there was a 25 % decrease in ATP hydrolysis rate (see Fig. S3). This result indicates that the PGK reaction is not the only reaction limiting the ATP hydrolysis rate, but that the thermal degradation activity and ATP recycling activity also contributed to the control of the ATP hydrolysis flux.

The analyses of PGK activity revealed quite different results for the 30 °C (yeast PGK) and 70 °C (*S. solfataricus* PGK) incubations. Whereas at 30 °C the thermodynamic constraints (highly positive ΔG^0) prevented an efficient conversion of 3 PG to BPG, at high temperatures there was an

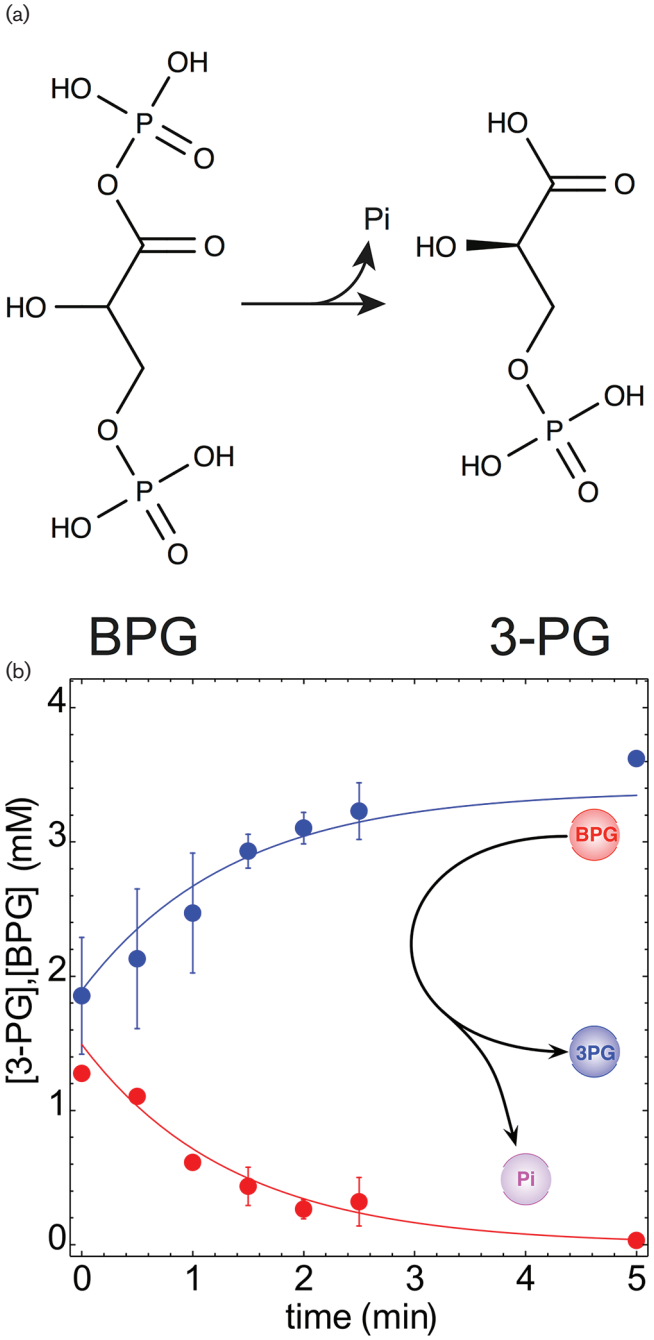

Fig. 2. BPG degradation to 3 PG at 70 °C. BPG produced with yeast PGK (Fig. 1a) was incubated at 70 °C, upon which BPG (red symbols) rapidly dephosphorylates to 3 PG (blue symbols). The drawn lines (coloured correspondingly to the symbols) show the exponential decay of BPG to 3 PG, simulated with a half-life time of 56.5 s (see Methods and the online Supplementary Material for details). Model simulations in Fig. 2(b) were made with the model kouril5.xml, and can be reproduced with the following link: https://jjj.bio.vu.nl/models/experiments/kouril2017_fig2b/simulate.

additional constraint as thermal degradation of BPG to 3 PG led to futile cycling of ATP. Nonetheless, both yeast and *S. solfataricus* are capable of a high gluconeogenic flux, carried by the PGK-GAPDH enzymes (see [9] for a theoretical analysis of the thermodynamics of the coupled system). We therefore tested experimentally whether coupling of PGK and GAPDH activities could overcome the thermodynamic constraint and protect against the futile cycling of ATP.

GAPDH catalyses a reductive dephosphorylation of BPG to GAP (see Fig. 4), and in combination with PGK this led to a complete conversion of 3 PG to GAP at 30 °C (Fig. 4b).

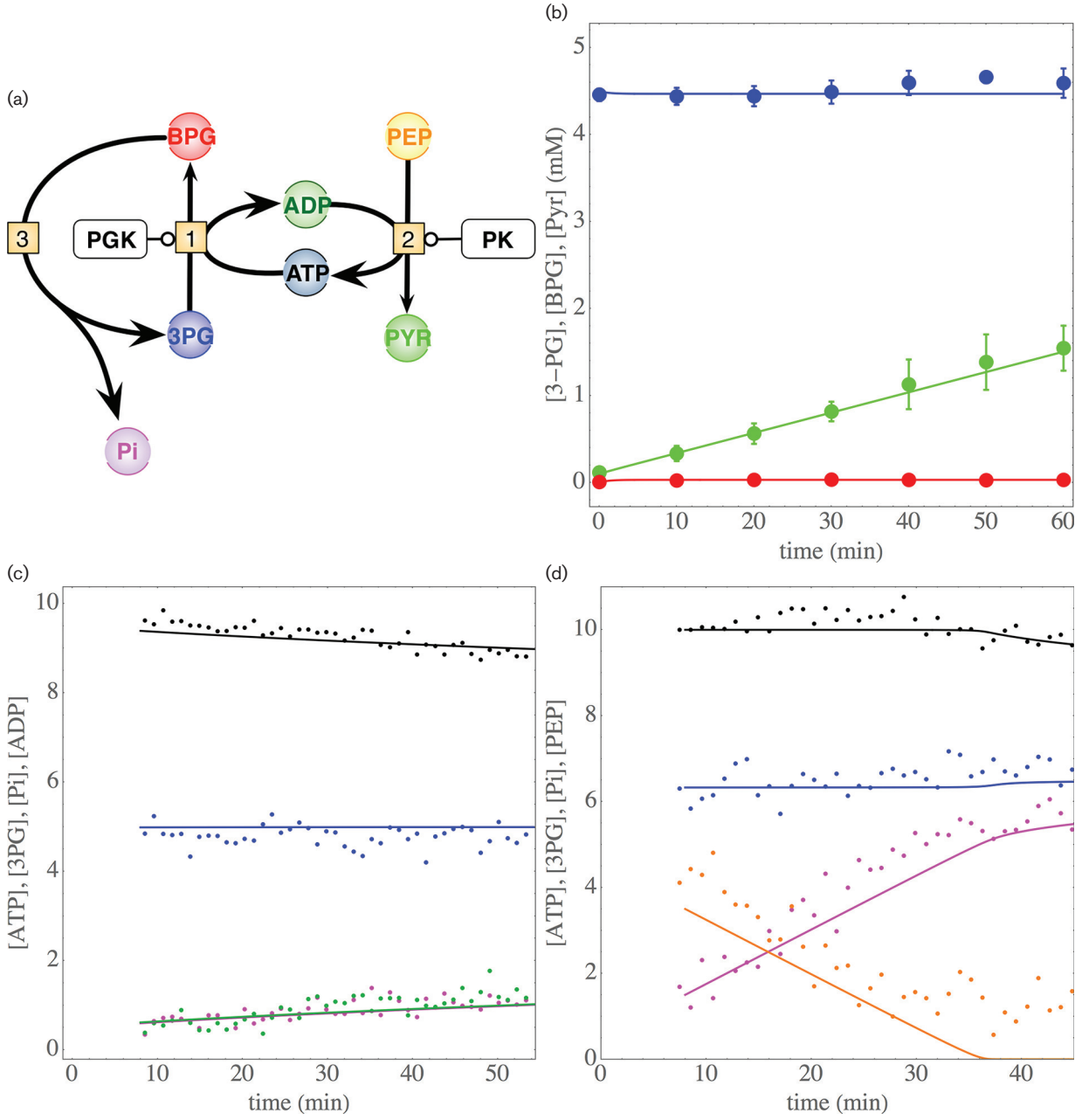

Fig. 3. PGK reaction at 70 °C. In Fig. 3(a) the reaction network for the system is shown; reaction 1 is catalysed by the PGK, reaction 2 is the ATP recycling reaction (PK), and reaction 3 is the thermal degradation of BPG. Fig. 3(b). *S. solfataricus* PGK (3.4 µg ml^{-1}) was incubated at 70 °C in the presence of the ATP recycling system and the conversion of 3 PG (blue symbols) to BPG (red symbols) was followed. Pyruvate (light green symbols) production via the ATP recycling system reflects ADP production. Similarly ^{31}P-NMR spectra, with additional metabolites ATP (black symbols), ADP (dark green symbols), PEP (orange symbols) and phosphate (pink symbols), are shown for *S. solfataricus* PGK (14 µg ml^{-1}) in the absence of the recycling system (Fig. 3c), and in the presence of ATP recycling (Fig. 3d, with 28 µg ml^{-1} SsoPGK). The lines (coloured correspondingly to the symbols) show the model predictions for the respective conditions (see Methods and the online Supplementary Material for details). Model simulations were made with the model kouril6.xml, and can be reproduced with the following links: https://jjj.bio.vu.nl/models/experiments/kouril2017_fig3b/simulate, https://jjj.bio.vu.nl/models/experiments/kouril2017_fig3c/simulate, https://jjj.bio.vu.nl/models/experiments/kouril2017_fig3d/simulate.

Thus, at moderate temperatures the thermodynamic constraint for PGK could be overcome by coupling its activity to GAPDH, and progress curves for the individual and combined reactions were in quantitative agreement with model predictions. For the incubation at 70 °C, we chose PGK concentrations such that 3 PG was expected to be

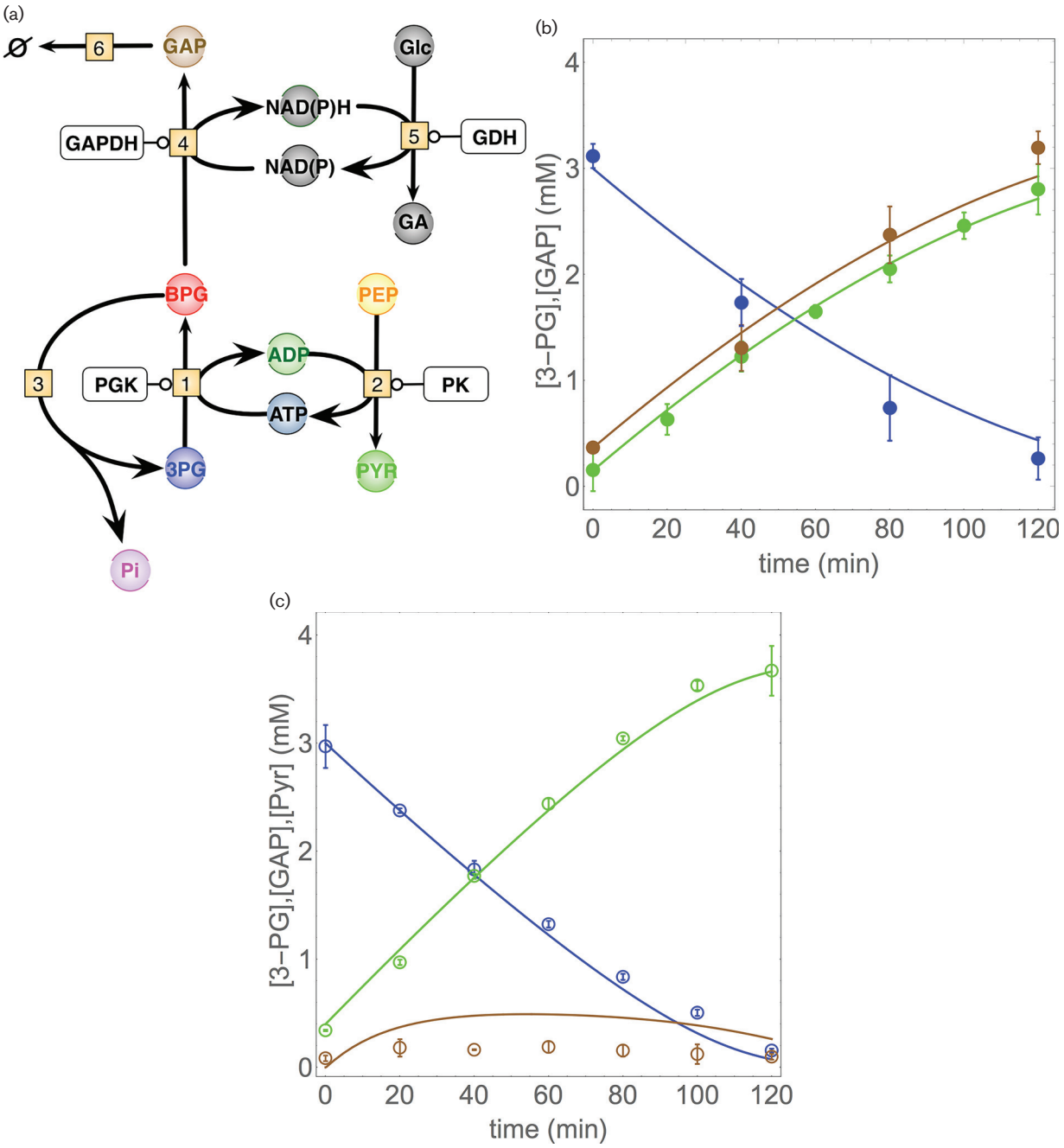

Fig. 4. Effect of temperature on the PGK-GAPDH reaction. The network structure for the PGK and GAPDH reactions and the co-factor recycling reactions are given in Fig. 4(a). Thermal degradation of BPG (reaction 3) and GAP (reaction 6) are only relevant for the 70 °C incubations. Combined incubations of PGK and GAPDH at 30 °C (Fig. 4b, yeast enzymes, closed symbols, 0.0324 µg ml^{-1} PGK and 0.052 mg ml^{-1} GAPDH) and at 70 °C (Fig. 4c, *S. solfataricus* enzymes, open symbols, 4.5 µg ml^{-1} PGK and 0.0421 mg ml^{-1} GAPDH) with the conversion of 3 PG (blue symbols) to GAP (brown symbols). Production of ADP is followed with pyruvate accumulation (light green symbols) via the co-factor recycling system. The lines in the figures (coloured correspondingly to the symbols) are model predictions for the respective systems (see Methods and the online Supplementary Material for details). Model simulations in Fig. 4(b, c) were made with the models kouril7.xml and kouril8.xml respectively, and can be reproduced with the following links: https://jjj.bio.vu.nl/models/experiments/kouril2017_fig4b/simulate, https://jjj.bio.vu.nl/models/experiments/kouril2017_fig4c/simulate.

consumed at a rate very close to the 30 °C incubation (while again saturating with GAPDH). Under these conditions 3 PG was indeed consumed rapidly, and futile cycling of ATP was almost zero (data not shown), but GAP concentrations were very low (Fig. 4b). The thermal instability of GAP at 70 °C leads to a different problem: GAP degrades

into compounds that are not part of gluconeogenesis, causing carbon loss from the system, and the formation of the toxic compound methylglyoxal at pH 7 [10]. Thus, coupling of PGK and GAPDH activities effectively overcomes the thermodynamic constraints on the PGK reaction and could solve the futile cycling at 70 °C, but temperature instability of GAP leads to carbon loss from the system. A high triose phosphate isomerase and fructose 1,6-bisphosphate aldolase/phosphatase activity can reduce the carbon loss by efficient conversion of GAP to thermostable fructose 6-phosphate [4].

In this manuscript we have focussed on the conversion of 3 PG to GAP via the PGK and GAPDH in an *in vitro* system using purified enzymes. We have shown that PGK in isolation acts as a futile cycle when incubated at 70 °C. The extent of futile cycling that occurs is dependent on the BPG concentration, and when PGK is incubated in combination with high GAPDH concentrations the futile cycling can be strongly reduced, as the BPG is kept low due to the high GAPDH activity. Thus, the extent of futile cycling is dependent on the relative activities of the PGK and GAPDH. This can be seen in the three incubations with different relative activities for PGK and GAPDH shown in Fig. S2. At high GAPDH/PGK ratios (12.4 : 1 in mass ratios) the 3 PG consumption in the PGK reaction is equal to the Pyr production in the ATP recycling reaction (Fig. 2a), this means that one ATP is consumed per 3 PG converted, i.e. no significant effect of futile cycling. At equal amounts of GAPDH and PGK (1 : 1 in mass ratios) the ATP consumption is roughly double the 3 PG consumption (Fig. S2e), indicating that half the BPG is cycled back to 3 PG. At low GAPDH/PGK ratios (0.35 : 1 in mass ratios) the ATP consumption rate is almost five times the 3 PG consumption rate (Fig. S2c), showing strong futile cycling.

Whereas the futile cycling rate is only dependent on the BPG concentration, which is set by the PGK/GAPDH ratio, the relative rate of futile cycling compared to the 3 PG to GAP conversion is also dependent on the total amount of PGK and GAPDH. The uncertainty of exact concentrations of PGK and GAPDH make it rather speculative to estimate the extent of futile cycling *in vivo*, but since it is not possible to directly measure this flux *in vivo*, an estimate based on the *in vitro* characterization is the best option. Based on specific activity measurements in cell free extracts [11], we estimate relative amounts of GAPDH and PGK of 1.20 and 1.74 mg/g cell extract. Assuming 250 mg prot ml^{-1} cytosol [11], this would give us intracellular concentrations of 300 and 436 μg ml^{-1} for GAPDH and PGK respectively. Thus, the relative amounts of GAPDH and PGK in the cytosol are close to the ratio we used in the incubation shown in Fig. S2 (e), but the *in vivo* concentrations are roughly 100-fold higher. When we simulate these conditions in our mathematical model we find that the futile cycling due to BPG degradation is approximately 3 % of the 3 PG conversion rate. Clearly, increasing the catalytic activity of PGK and GAPDH, but not the chemical degradation of BPG makes the relative contribution of the futile cycling smaller, but a 3 % futile cycling effectively means that the PGK-GAPDH reactions consume 1.03 moles of ATP to convert 1 mole of 3 PG to GAP. This might put a significant burden on cellular physiology, specifically when taking into account that many other intermediates might be temperature sensitive (e.g. GAP and DHAP in the glycolytic pathway).

In (hyper)thermophilic Archaea, the metabolic pathways are often very similar to the pathways used in mesophilic organisms. The adaptations to life at high temperature have not been at the pathway level, but more at the catalyst level. Although several enzymes catalyse unusual reactions, e.g. in glycolysis there is a non-phosphorylating glyceraldehyde-3-phosphate dehydrogenase (GAPN) and glyceraldehyde-3-phosphate:ferredoxin oxidoreductase (GAPOR), which catalyse the direct oxidation of GAP to 3 PG [1, 12–14], this is a local effect, as the product 3 PG is again an intermediate of the main pathway. The net effect of bypassing the unstable BPG is loss of substrate-level phosphorylation via PGK. The GAPN and GAPOR could represent a special adaptation strategy to bypass thermal labile intermediates such as BPG [9, 12]. However, detailed enzyme characterizations as well as knock-out studies revealed that the PGK-GAPDH enzyme couple is functional and essential for anabolism in hyperthermohilic Archaea [4, 14]. In a recent review [15], the consequences of largely overlooked spontaneous chemical reactions in metabolism and damaging side reactions of enzymes were discussed. Clearly, degradation of metabolites is more dramatic at higher temperatures and can cause a large burden due to carbon loss, formation of toxic metabolites like methylglyoxal [10], and dephosphorylation of phosphorylated intermediates leading to futile cycling of ATP.

Funding information
We acknowledge the financial assistance of the Biotechnology and Biological Sciences Research Council, UK (JLS via BBG0102181, BB/I004637/1, BB/M013189/1), BMBF (TK and BS via SulfoSYSBIOTECH 0316188A) and NRF/DST, DST/NRF (SARCHI) in South Africa (JLS and JE via NRF-SARCHI-82813).

Conflicts of interest
The authors declare that there are no conflicts of interest.

References

1. Bräsen C, Esser D, Rauch B, Siebers B. Carbohydrate metabolism in Archaea: current insights into unusual enzymes and pathways and their regulation. *Microbiol Mol Biol Rev* 2014;78:89–175.
2. Sato T, Atomi H. Novel metabolic pathways in Archaea. *Curr Opin Microbiol* 2011;14:307–314.
3. Zampar GG, Kümmel A, Ewald J, Jol S, Niebel B *et al.* Temporal system-level organization of the switch from glycolytic to gluconeogenic operation in yeast. *Mol Syst Biol* 2013;9:651.
4. Kouril T, Esser D, Kort J, Westerhoff HV, Siebers B *et al.* Intermediate instability at high temperature leads to low pathway efficiency for an in vitro reconstituted system of gluconeogenesis in *Sulfolobus solfataricus*. *FEBS J* 2013;280:4666–4680.
5. Teusink B, Passarge J, Reijenga CA, Esgalhado E, van der Weijden CC *et al.* Can yeast glycolysis be understood in terms of in vitro kinetics of the constituent enzymes? Testing biochemistry. *Eur J Biochem* 2000;267:5313–5329.

6. **Wolfram Research Inc.** *Mathematica Edition: Version 11.0*. Champaign, Illinois: Wolfram Research, Inc; 2016.
7. **Schramm A, Kohlhoff M, Hensel R.** Triose-phosphate isomerase from *Pyrococcus woesei* and *Methanothermus fervidus*. *Methods Enzymol* 2001;331:62–77.
8. **Haferkamp P.** Biochemical studies of enzymes involved in glycolysis of the thermoacidophilic crenarchaeon *Sulfolobus solfataricus*. PhD-thesis, Universitaet Duisburg-Essen, Essen; 2011.
9. **Zhang Y, Kouril T, Snoep JL, Siebers B, Barberis M *et al.*** The peculiar glycolytic pathway in hyperthermophylic archaea: understanding its whims by experimentation *In* Silico. *Int J Mol Sci* 2017;18:876.
10. **Gauss D, Schoenenberger B, Wohlgemuth R.** Chemical and enzymatic methodologies for the synthesis of enantiomerically pure glyceraldehyde 3-phosphates. *Carbohydr Res* 2014;389:18–24.
11. **Figueiredo AS, Kouril T, Esser D, Haferkamp P, Wieloch P *et al.*** Systems biology of the modified branched Entner-Doudoroff pathway in *Sulfolobus solfataricus*. *PLoS One* 2017;12:1–25.
12. **Ettema TJ, Ahmed H, Geerling AC, van der Oost J, Siebers B.** The non-phosphorylating glyceraldehyde-3-phosphate dehydrogenase (GAPN) of *Sulfolobus solfataricus*: a key-enzyme of the semi-phosphorylative branch of the Entner-Doudoroff pathway. *Extremophiles* 2008;12:75–88.
13. **Brunner NA, Brinkmann H, Siebers B, Hensel R.** NAD^+-dependent Glyceraldehyde-3-phosphate dehydrogenase from *Thermoproteus tenax*. *J Biol Chem* 1998;273:6149–6156.
14. **Matsubara K, Yokooji Y, Atomi H, Imanaka T.** Biochemical and genetic characterization of the three metabolic routes in *Thermococcus kodakarensis* linking glyceraldehyde 3-phosphate and 3-phosphoglycerate. *Mol Microbiol* 2011;81:1300–1312.
15. **Linster CL, van Schaftingen E, Hanson AD.** Metabolite damage and its repair or pre-emption. *Nat Chem Biol* 2013;9:72–80.

Edited by: S-V. Albers and F. Sargent